NAVSWC TR 91-640

A PVDF TRIGGER AND TILT DETECTOR FOR PROJECTILE IMPACT EXPERIMENTS

BY DOUGLAS G. TASKER, PAUL K. GUSTAVSON, AND WILLIAM H. WILSON

RESEARCH AND TECHNOLOGY DEPARTMENT

NOVEMBER 1991

NAVAL SURFACE WARFARE CENTER

Dahlgren, Virginia 22448-5000 • Silver Spring, Maryland 20903-5000

A PVDF TRIGGER AND TILT DETECTOR FOR PROJECTILE IMPACT EXPERIMENTS

BY DOUGLAS G. TASKER, PAUL K. GUSTAVSON,
AND WILLIAM H. WILSON

RESEARCH AND TECHNOLOGY DEPARTMENT

NOVEMBER 1991

NAVAL SURFACE WARFARE CENTER
Dahlgren, Virginia 22448-5000 • Silver Spring, Maryland 20903-5000

FOREWORD

This report describes the design and use of a piezoelectric polymer, polyvinylidene di-fluoride (PVDF), as a sensor for the measurement of projectile tilt, and as a trigger source for shock wave and projectile impact experiments. The one device produces two independent signals: one a piezoelectric signal, the other a contact-closure signal. This duality significantly improves the reliability of the trigger; if one signal fails then the other will still be available.

Analyses are provided to allow the prediction of signal magnitudes from both the shocked PVDF mode and the contact-closure mode of the trigger sensor.

Experimental details are given for both the physical and electrical construction of the trigger sensor so that this work can be applied in future research.

Results from the use of this device, obtained in impact experiments, are presented that demonstrate the advantages of the trigger. To date this trigger has been used successfully by the authors many times without a single failure.

Approved by:

WILLIAM H. BOHLI, Acting Head
Energetic Materials Division

Accession For	
NTIS GRA&I	☑
DTIC TAB	☐
Unannounced	☐
Justification	
By	
Distribution/	
Availability Codes	
Dist	Avail and/or Special
A-1	

CONTENTS

ILLUSTRATIONS

TABLES

CHAPTER 1

INTRODUCTION

THE DUAL TRIGGER SOURCE

A reliable trigger source is crucial to any single-shot shock wave, or projectile impact, experiment involving electrical diagnostics. A good trigger source is one that consistently provides a predictable signal with a fast rise time, and is not prone to receiving stray signals from outside sources. The addition of a second, nearly simultaneous, triggering mechanism provides further confidence that cameras, oscilloscopes, pulsers, etc., will be triggered correctly and reliably during an experiment. To date the trigger sensor described here has been used successfully many times without a single failure.

This report details the design of a trigger source that produces two nearly simultaneous pulses using two independent techniques on the one sensor. One pulse is piezoelectrically generated by shocking the thin PVDF sensor. This piezoelectric signal is a precursor to a closing switch signal, which is produced by using the same sensor as the closing switch in a capacitor discharge circuit. The rise time and magnitude of the piezoelectric precursor depends on the radius, impact velocity, and tilt of the projectile. By contrast, the closing switch signal is independent of the projectile parameters.

The generation of two signals from one source results in a high trigger reliability. The circuitry required is simple, and the combined sensor and circuit is inexpensive.

PROJECTILE TILT MEASUREMENT

The projectile impact experiments described here are fairly typical of such experiments. A steel cylinder is projected by a gun towards a target at a prescribed velocity and strikes at a particular impact (tilt) angle. It is frequently important to know the angle between the projectile and the target on impact, i.e., the tilt angle. We will describe the measurement of tilt angle using a PVDF sensor. Up to now the tilt angle could only be measured with a high-speed framing camera, a technique that is difficult, expensive, inaccurate, and only suitable for laboratory conditions.

We will show how a polyvinylidene di-fluoride (PVDF) sensor can be used to measure tilt angle, and how it can also be used as a reliable impact trigger. The method is simple and inexpensive.

PVDF AS A STRESS TRANSDUCER

Properly prepared sheets of PVDF polymer exhibit excellent piezoelectric properties. PVDF film products typically generate large electrical signals when shocked. PVDF is a long-chain semicrystalline polymer containing repeating units of CH_2-CF_2. During manufacture, a non-polar, so-called α-phase material is produced. By stretching the film while it cools, a polar or ß-phase PVDF is created. The film is metallized on each side with a desired pattern and then subjected to a large electric field (circa 10^8 V/m), which aligns the ß-phase crystallites, resulting in a permanent polarization. It is this metallized, poled, ß-phase PVDF that is used for making piezoelectric film products. Depending on the techniques used in the above processes, anything from high quality, precision shock pressure transducer elements to inexpensive stress sensors can be made.

Stress transducers manufactured from PVDF must be used with caution; the PVDF material must be correctly manufactured to give it a predictable performance. PVDF transducers obtained from some manufacturers produce an electrical charge, as a function of pressure, which is significantly non-linear, even parabolic. The sensitivity of the device is also a strong function of the source of the virgin polymer and of the methods of stretching and poling. Bauer[1] has patented a poling technique that minimizes non-linearities and produces reproducible, precision stress transducers. These precision transducers are commercially available; they are manufactured from a master batch of PVDF virgin polymer, poled with the Bauer process, and distributed in the US by Ktech.* Poling data for each of these transducers are supplied by the manufacturer.

For this work Kynar LDT1-028K PVDF film sensors** were used (Figure 1-1). These sensors were 208 μm thick and comprised of a 28 μm thick PVDF film, a 125 μm thick protective Mylar backing, and adhesive. These particular sensors are manufactured with twisted-pair leads connected. Where the thickness is crucial DT1-028K sensors may be used; they are 28 μm thick and have no protective backing and no leads. Like all PVDF products, they are very flexible, which makes them unobtrusive and easy to mount on targets. Kynar sensors are not recommended for precision pressure measurement, but are suitable for many other applications including the trigger and tilt sensors described here. They are inexpensive and can be obtained in relatively large sizes, e.g., gauges with dimensions of 165 mm × 22 mm.

The output signal characteristics (magnitude and rise time) depend upon the shock loading and how the sensors are connected in a circuit; this is discussed in Chapter 2. The discussion of the application of these sensors as triggering devices in projectile impact experiments is included in subsequent chapters.

---

*Ktech Corporation, 901 Pennsylvania Ave. NE, Albuquerque, NM 87110.

**Pennwalt Corporation, Piezo Film Sensor Division, P.O. Box 799, Valley Forge, PA 19482.

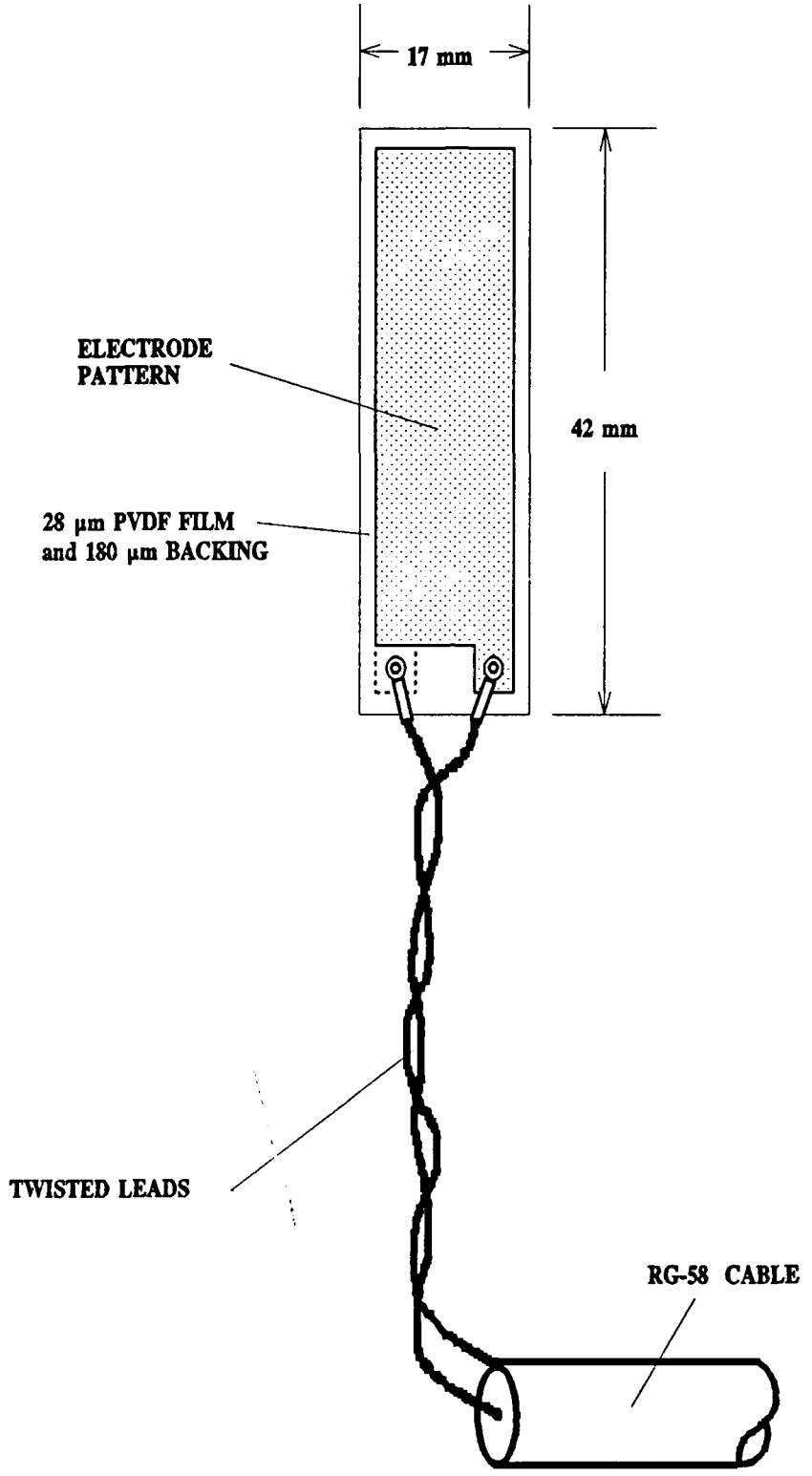

FIGURE 1-1. PVDF SENSOR AND CABLE

In the following chapters the electrical design of the trigger is described, and the techniques for predicting trigger signal magnitudes and rise times are provided. The sensor's electrical response is analyzed in two parts: first the piezoelectric response, then the contact-closure response. The combined trigger is discussed in Chapter 2. Appendix A briefly describes the overall experimental arrangement used in this work.

CHAPTER 2

THE MEASUREMENT OF PROJECTILE TILT

In this chapter the measurement of projectile tilt and the electrical design of the piezoelectric trigger are described. In the analysis it is assumed that the projectile travels ***in vacuo***, i.e., the effects of the projectile's travel through a gas at atmospheric pressure are ignored. Thus, any effects from a bow wave attached to the projectile are not considered. The effects of a bow wave, if any, should be the subject of future work. The criteria for a good trigger include a fast rise time signal and a predictable signal magnitude.

The circuit of a piezoelectric PVDF trigger is modeled in Figure 2-1; the combined circuit is discussed in Chapter 4. The Kynar LDT1-028K sensor had outer dimensions of nominally 40 mm × 15 mm; the 3.81 cm^2 active area, A, of the sensor had a measured capacitance of 1.1 nF at 10 kHz, which corresponds to a relative dielectric constant, ϵ, of 9.14. We now consider the signal generated by the impact of a cylindrical projectile. Note that the analysis for the output signal, Equation (2-10), can be used for projectiles of any shape of impact surface.

ANALYSIS

TABLE 2-1. DATA FOR EXAMPLE

C	Sensor capacitance	1.1 nF
A	Sensor active area	3.81 cm^2
d	PVDF film thickness	28 μm
ϵ	Sensor relative dielectric constant	9.14
r	Projectile radius	4.763 mm
v_p	Projectile velocity	500 m/s
θ	Projectile tilt	20 mrads

The area impacted by a 9.525 mm diameter projectile would be 71.26 mm^2 if the impact were planar, i.e., without tilt. The area of the PVDF sensor that would be impacted therefore has a capacitance of C_1 = 206 pF, and it shares the piezoelectric charge with the remaining sensor area of capacitance, C_2, C_2 = 1.1 nF - 206 pF or 894 pF. In practice the projectile will impact the sensor at a small angle, θ, so that the area of impact, $A(t)$, is initially zero and rises to the full area, πr^2, during the period of impact. Assuming no deceleration during the initial stages of impact, the total duration of impact is given by the

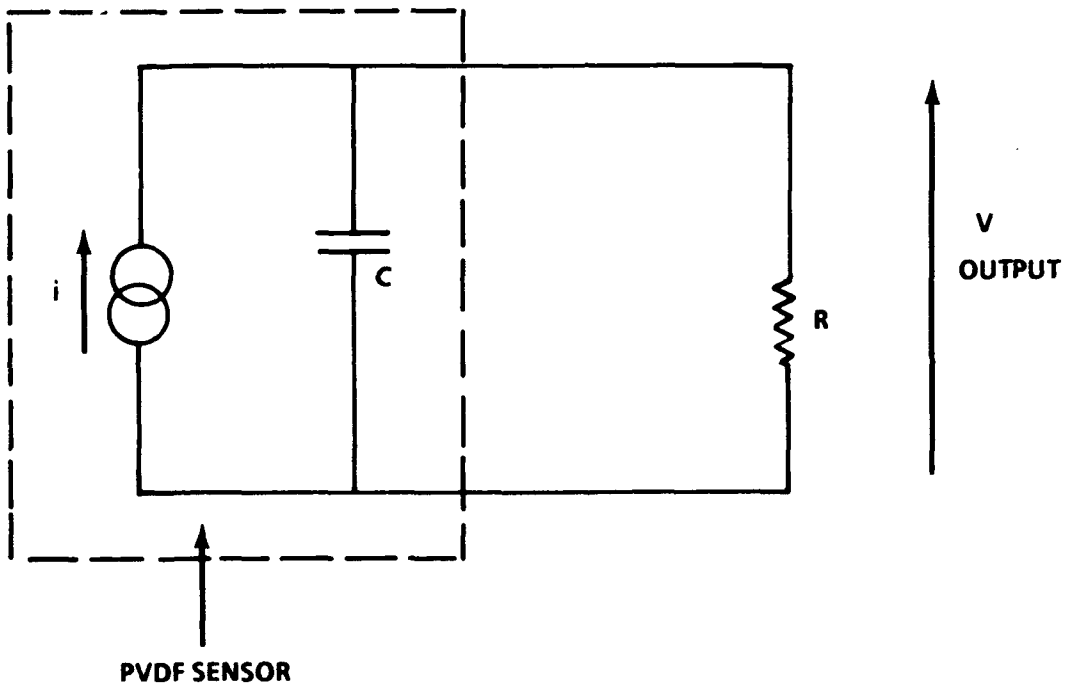

FIGURE 2-1. SCHEMATIC OF PVDF PIEZOELECTRIC TRIGGER CIRCUIT

time for the full area of contact to be achieved, t_f

$$t_f = \frac{2r\theta}{v_p} \tag{2-1}$$

where r is the projectile radius and v_p, the projectile velocity. Now the area of impact, $A(t)$, can be expressed in terms of α, i.e., the angle subtended between the radius and a chord at the front of the impact area (Figure 2-2). We define α thus:

$$\cos\alpha = 1 - \frac{v_p t}{r\theta} \tag{2-2}$$

At the time, t, the change of area, dA, can be expressed as 2r sin α dx, and so

$$dx = r\sin\alpha\, d\alpha = \frac{v_p}{\theta} dt \tag{2-3}$$

hence

$$\begin{aligned} dA(t) &= 2r\sin\alpha\, dx \\ &= 2r\sin\alpha \times r\sin\alpha\, d\alpha \\ &= r^2(1-\cos 2\alpha)\, d\alpha \end{aligned} \tag{2-4}$$

The total area of impact at some time after first contact is found by integrating from the start of impact to the angle α, where α is defined by Equation (2-2); thus,

$$\begin{aligned} A(t) &= r^2 \int_0^{\alpha} (1-\cos 2\phi)\, d\phi \\ &= r^2\left(\alpha - \frac{\sin 2\alpha}{2}\right) \end{aligned} \tag{2-5}$$

The magnitude of the impact area, $A(t)$, as a function of time is shown in Figure 2-3.

Now the current generated by the PVDF sensor can be expressed as the rate of change of the charge, the product of the charge density and the area, ρA. The resultant voltage, V, is developed by the sensor across the resistor, R. The current is the sum of the currents in the capacitor, C, and resistor, R,

$$i = C\frac{dV}{dt} + \frac{V}{R} \tag{2-6}$$

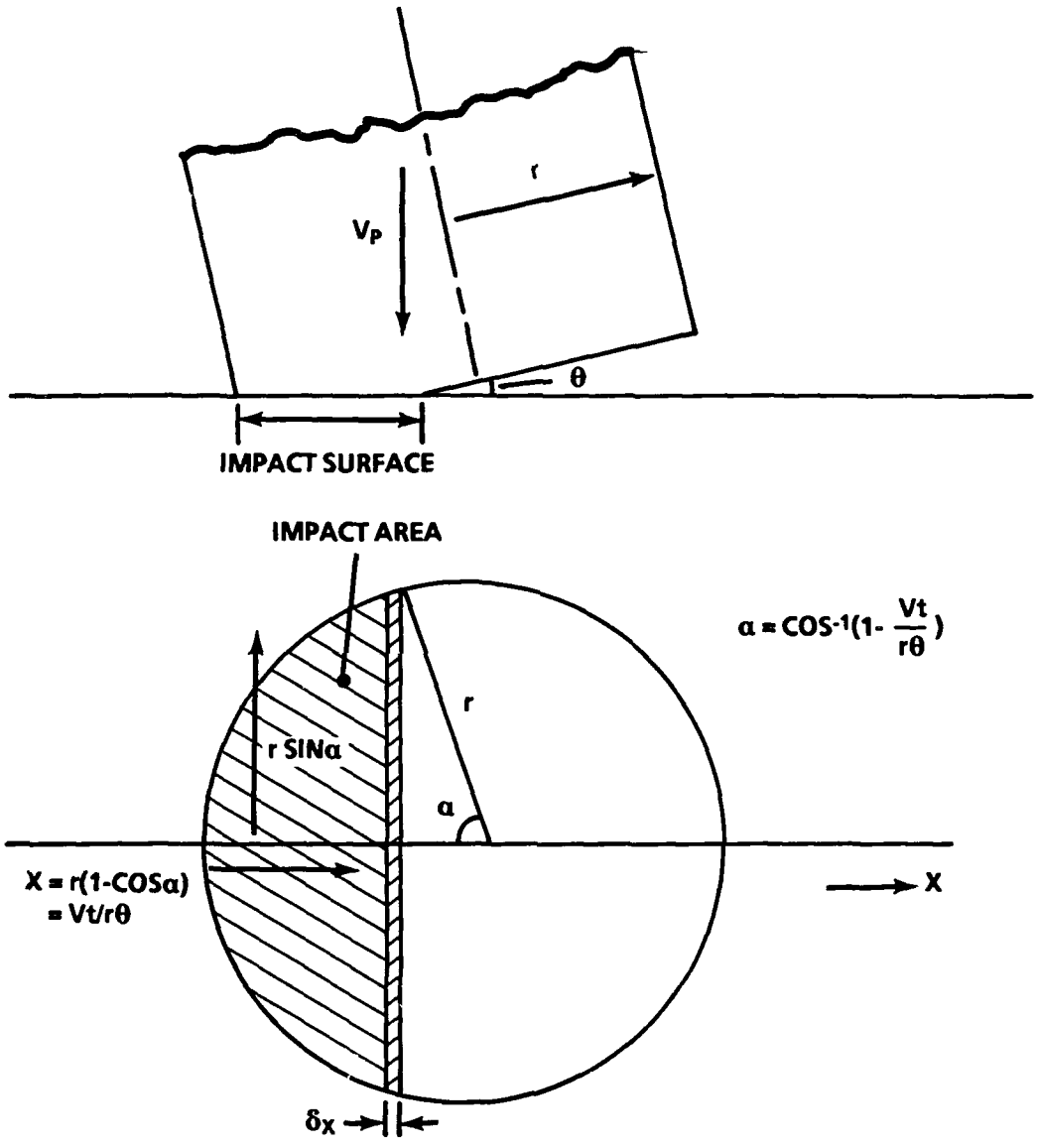

FIGURE 2-2. METHOD OF CALCULATING IMPACT AREA

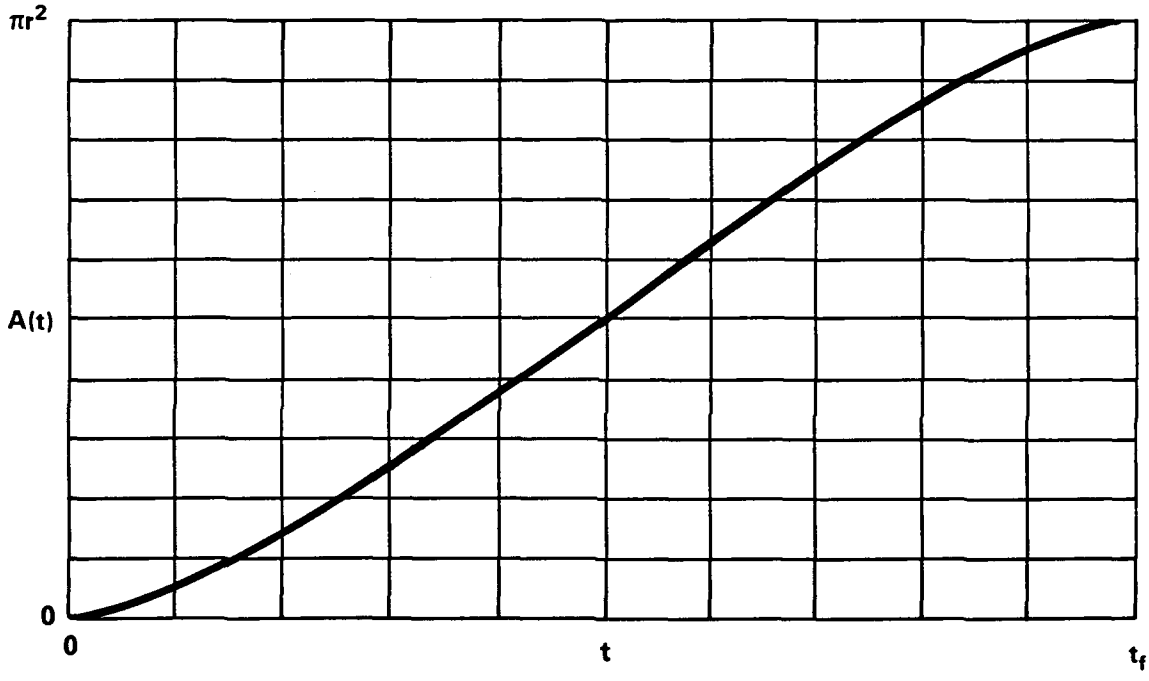

FIGURE 2-3. IMPACT AREA A(t) VERSUS TIME

The solution to this differential equation is

$$V(t) = \frac{1}{C} e^{\frac{-t}{CR}} \int_0^t i(t) e^{\frac{+t}{CR}} dt \tag{2-7}$$

This solution can be verified by substitution into Equation (2-6).

We assume that the pressure pulse can be represented by a step rise to a pressure P_{max}. By implication the shock ring-up time in the PVDF is assumed to be negligible. The resultant charge density (electrical charge per unit area) on the sensor will also be a step, $\rho = \rho(P_{max})$. We assume that C is constant with time; if d is the PVDF film thickness then C is given by

$$C = \frac{\epsilon \epsilon_0 A}{d} \tag{2-8}$$

If ρ is constant, i.e., a function only of pressure, $\rho(P)$, then we write ρ for simplicity and the current can be expressed as a function of area, i.e.,

$$\begin{aligned} i(t) &= \frac{d(\rho A)}{dt} = \rho \frac{dA(t)}{dt} + A(t) \frac{d\rho}{dt} \\ &= \rho \frac{dA(t)}{dt} \end{aligned} \tag{2-9}$$

Here $A(t)\ d\rho/dt$ is always zero for a step-shock (flat-topped). Now the full solution to the output voltage can be expressed as a function of incremental area:

$$V(t) = \frac{\rho}{C} e^{\frac{-t}{CR}} \int_0^t \frac{dA(t)}{dt} e^{\frac{+t}{CR}} dt \tag{2-10}$$

Note that for a step-shock the structure of the $\rho(P)$ calibration does not affect the structure of the output signal in Equation (2-10), only its magnitude. Substituting Equations (2-3) and (2-4) for dt and dA/dt, and substituting γ for $v_p t/r\theta$, we have V(t) as a function of tilt angle θ:

$$\begin{aligned} V(t) &= \frac{2\rho r v_p}{C\theta} e^{\frac{-t}{CR}} \int_0^t \sin\alpha\, e^{\frac{+t}{CR}} dt \\ &= \frac{2\rho r^2}{C} e^{\frac{-t}{CR}} \int_0^t \sqrt{2\gamma - \gamma^2}\ e^{\frac{+r\theta}{CRv_p}\gamma} d\gamma \end{aligned} \tag{2-11}$$

Equation (2-11) is the exact solution for the piezoelectric signal.

Calibration data

There are no calibration data available for the Kynar sensor in terms of $\rho(P)$ in this pressure range. For purposes of illustration, we have used the calibration data for the Bauer transducer reported by Graham[2] and Moore.[3] The Bauer polymer is probably of a different sensitivity than the Kynar material. These data are for a 'shorted' piezoelectric sensor, i.e., the electric field across the sensor is kept small by shunting it with a small impedance. Under these conditions the electric charge density, ρ, is directly proportional to stress.

The calculation would be precise if a Bauer-type sensor were used. For ease of analysis we have fitted a power law to the Graham and Moore data.

$$\rho(P) = kP^{\beta} \tag{2-12}$$

Here k = 1.0025, β = 0.6046, P is in GPa, and $\rho(P)$ is in $\mu C/cm^2$.

Numerical solution

An analytic solution to Equation (2-11) has not been found. The solution can be obtained numerically, as shown in Figure 2-4, where the predicted output signal is shown for an impact pressure of P_{max} = 2.87 GPa and $\rho(P_{max})$ = 1.896 $\mu C/cm^2$. The pressure of 2.87 GPa corresponds to the impact of a mild steel projectile against an explosive (Pentolite) at 500 m/s; for mild steel impacting mild steel, P_{max} = 8.0 GPa. P_{max} was obtained using conventional shock impedance mismatch calculations. The resistance R = 50 Ω, and the other pertinent data for this example are taken from Table 2-1.

Shock ring-up in PVDF

The PVDF sensor is sandwiched between the projectile and the target from the time of impact. However, we have ignored the effect of the sensor on the impact pressure because the sensor is thin. In other words, the shock reverberation time (ring-up) of a 208 μm thick Kynar LDT1-028K package is $\approx$100 ns; the PVDF and the backing of the Kynar sensor are of similar shock impedances to most explosives so that the total ring-up time will be close to 100 ns. Note that the sweep time of a 12.7 mm diameter projectile impacting with a velocity of 500 m/s at an angle of 1° is 141 ns.

For steel to steel impacts the shock impedance of the sensor package is significantly mismatched to the steel, so the ring-up could be 1 μs with the 208 μm thick sensor.

Penetration of sensor

The piezoelectric signal can be interrupted at any time by the switch closure signal due to eventual projectile penetration of the sensor. This complication will be discussed later. The sensing circuit components can be chosen to simplify the analysis, i.e., when certain simplifying assumptions become valid. These correspond to the so-called "charge mode" and "current mode" circuit designs.

Output voltage for large values of resistance, charge mode

If the resistor R is large so that the current in R is negligible compared to the current in the capacitor C, then Equation (2-6) can be simplified,

$$i \approx C\frac{dV}{dt} \tag{2-13}$$

Following the same procedure as above we find

$$V(t) \approx \frac{\rho}{C}A(t) \tag{2-14}$$

Equation (2-14) describes what is termed the "charge mode" of operation because the output is directly proportional to the charge ρ. The solution is identical to the solution for small times, i.e., $t \ll CR$. The maximum output voltage occurs at t_f when $V = \pi r^2 \rho/C$. Figure 2-5 shows the calculated waveforms for $CR = 10\ \mu s$ ($R = 50\ \Omega$, $C = 0.2\ \mu F$) using the exact and approximate solutions, i.e., Equations (2-11) and (2-14). The agreement between the two equations is quite good. Note that C has been increased from 1.1 nF to 0.2 μF, to satisfy the inequality, by placing an additional capacitance in parallel with the resistor. As with all high frequency circuits, great care must be taken to use high frequency (low inductance) capacitors and resistors, and to keep lead inductances small; otherwise, high frequency oscillations and erroneous data will be obtained.

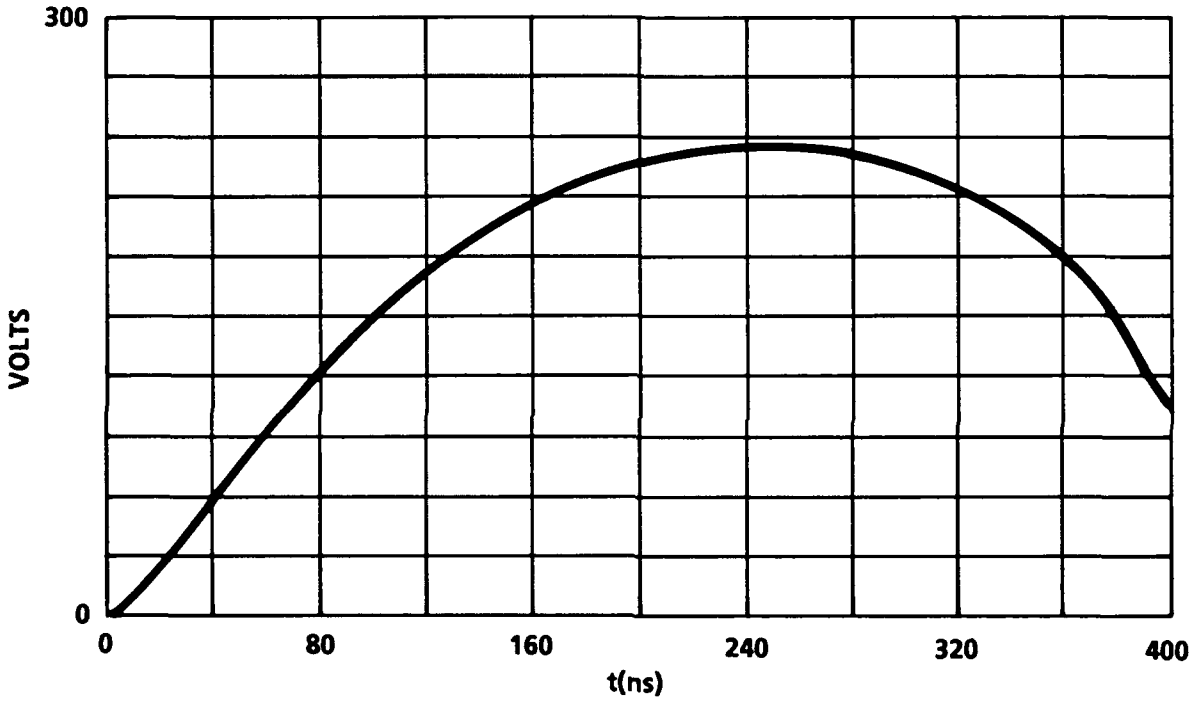

FIGURE 2-4. PIEZOELECTRIC SIGNAL, CR = 55 ns, EQUATION (2-11)

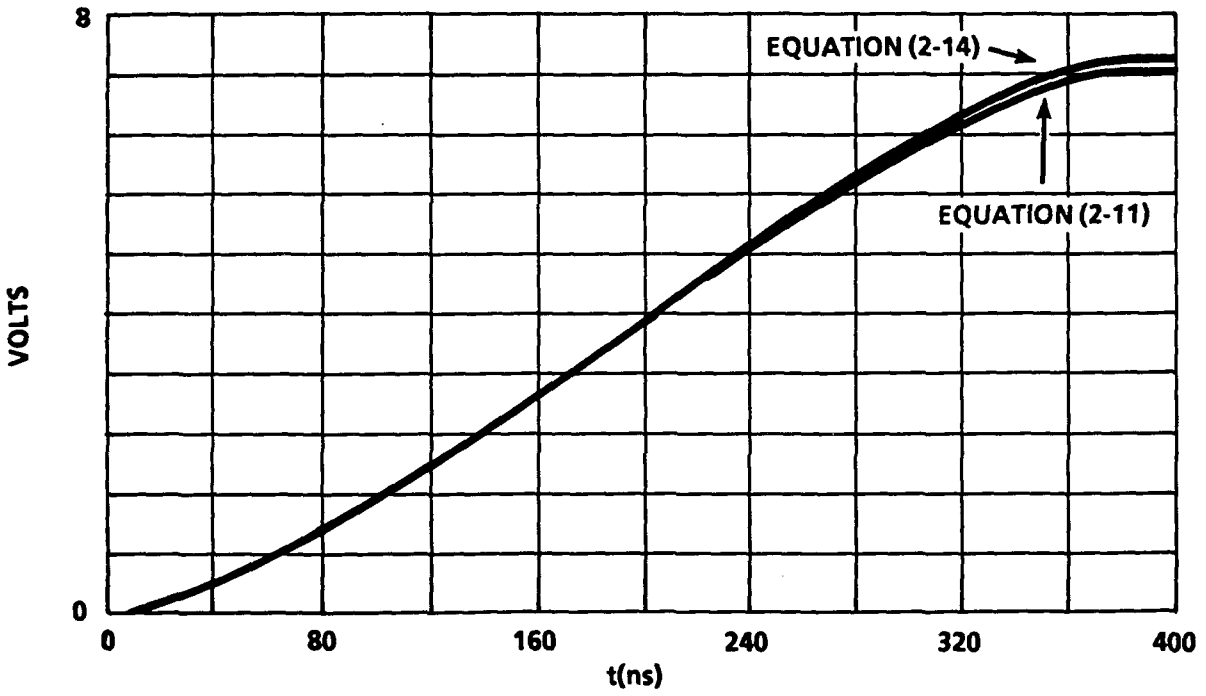

FIGURE 2-5. SIGNALS FOR CR = 10 μs, CHARGE MODE, EQUATIONS (2-11) AND (2-14)

Output voltage for small values of resistance, current mode

If the resistor, R, is small, so that the current in C is negligible compared to the current in R, then Equation (2-6) is simplified again,

$$V(t) \approx i(t)R = \rho R\frac{dA}{dt} \tag{2-15}$$

then from Equations (2-3), (2-4), and (2-9), where $\gamma = v_p t/r\theta$,

$$\begin{aligned} V(t) &\approx \frac{2\rho r v_p R}{\theta}\sin\alpha \\ &\approx \frac{2\rho r v_p R}{\theta}\sqrt{2\gamma - \gamma^2} \end{aligned} \tag{2-16}$$

Equation (2-16) describes the so-called "current mode" of operation because the output is directly proportional to the current in the PVDF sensor. The solution is circular, i.e., $V(t) \propto \sin\alpha$, $t \propto (1 - \cos\alpha)$. Here the maximum voltage occurs at $t = t_f/2$ when $\sin\alpha = 1$ and $V = 2\rho r v_p R/\theta$; see Figure 2-6 where CR = 1.1 ns, R = 1 Ω, and C = 1.1 nF. Although the figure shows the solutions for both Equations (2-11) and (2-16), the solutions are in such close agreement that the two plots are indistinguishable.

Pseudo-current mode

The accuracy of Equation (2-16) is reasonably good even when the time, t, is comparable to CR, i.e., the condition that t is much greater than CR is not satisfied. For example, the solution of Figure 2-4, where CR = 55 ns and $0 < t < 400$ ns, has been recalculated with Equation (2-16) and is shown in Figure 2-7. The peak voltages of the two solutions differ by only 4 percent, although they are shifted in time relative to each other. Consequently, Equation (2-16) is useful to predict approximate signal magnitudes, or to calculate approximate tilt angles over a wide range of values for CR in the "current mode."

CALCULATION OF TILT FROM THE PIEZOELECTRIC SIGNAL

Equations (2-14) and (2-16) show how r, v_p, R, C, and θ, affect the signal magnitude and structure. Whenever possible the sensor should be operated in the "current mode." In this mode no additional capacitor is required and the peak voltage, as predicted by Equation (2-16), is inversely proportional to θ. Nevertheless, in either mode, the measurement of the voltage profile provides sufficient information to calculate the tilt.

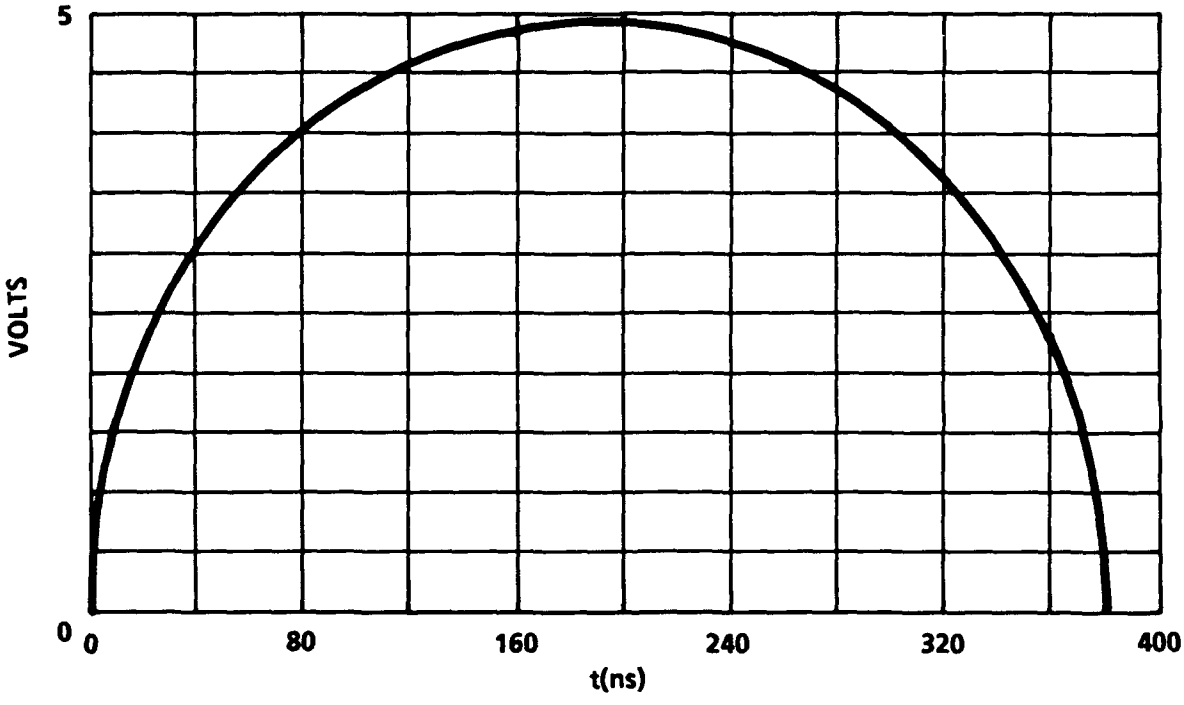

FIGURE 2-6. SIGNALS FOR CR = 1.1 ns, CURRENT MODE, EQUATIONS (2-11) AND (2-16)

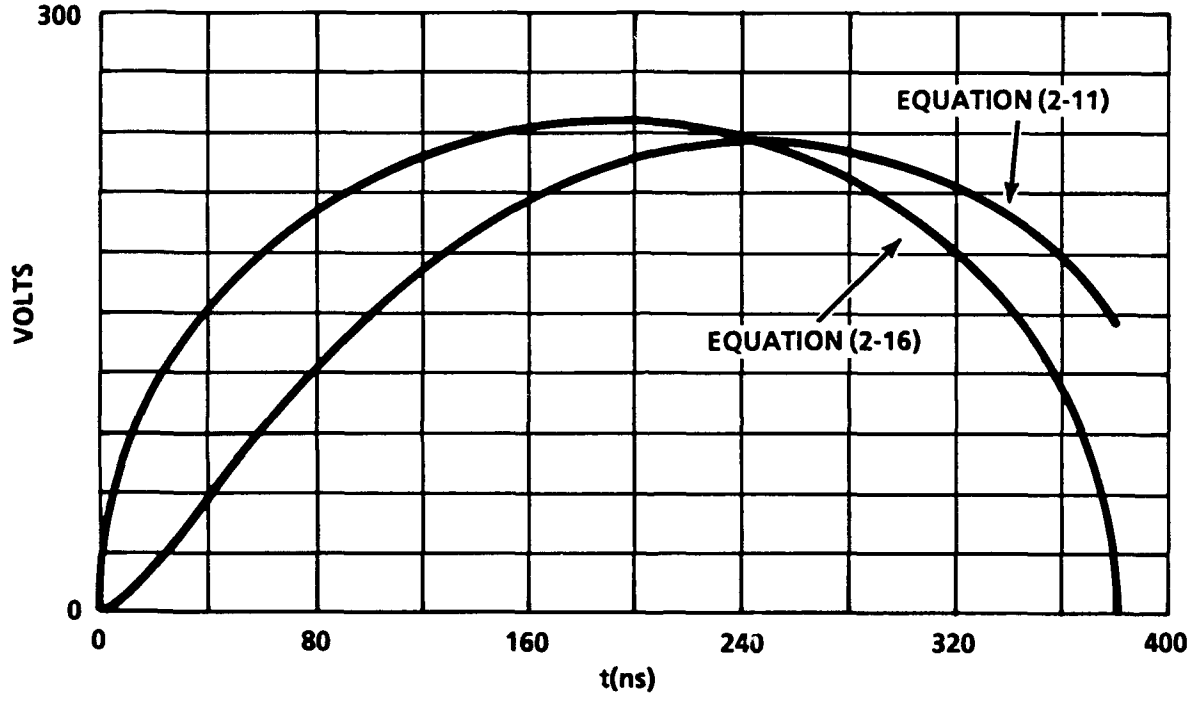

FIGURE 2-7. SIGNALS FOR CR = 55 ns, PSEUDO-CURRENT MODE, EQUATIONS (2-11) AND (2-16)

PENETRATION OF SENSOR BY PROJECTILE

The piezoelectric signal may be interrupted due to penetration by the projectile through the sensor. At that instant the charge $\rho(P)$ is discharged, because the projectile short-circuits the sensor, and the signal rapidly decays to zero. This feature would ordinarily be undesirable. However, it can be exploited if the sensor is wired as a closing switch, i.e., in addition to being wired as a piezoelectric gauge. This is described in Chapter 3.

CHAPTER 3

THE CLOSING SWITCH TRIGGER CIRCUIT

The closing switch here is effected by the penetration of the projectile through the PVDF sensor. This penetration creates a short-circuit between the two surfaces of the sensor and completes the circuit. The penetration also discharges the piezoelectric charge developed across the sensor capacitance. The analysis that follows is equally applicable to any closing switch mechanism. Such devices may include ionization pins, crushing switches, make-screens, and so on.

A basic closing switch trigger is shown in Figure 3-1. The capacitor, C_c, is charged to the supply voltage, V_c, via a large charging resistor, R_c. Note that C_c is not the capacitance formed by the sensor. The inductance, L, represents the stray inductance of the closing circuit. It will be shown that it is essential that L is kept small for efficient circuit operation. Resistor, r, is the load resistance connected across the device to be triggered, e.g., an oscilloscope. This load resistance must match the impedance of the connecting coaxial cable, i.e., 50 Ω for a 50 Ω cable.

CLOSING SWITCH CIRCUIT SOLUTION

Using conventional circuit theory we equate the sum of the voltages in the circuit to the voltage on the capacitor, V_c. If time t = 0 represents the time when the switch is closed we have

$$\frac{1}{C_c}\int_0^t i\,dt + L\frac{di}{dt} + ir = V_c \qquad (3\text{-}1)$$

The classic solution to this series LCR circuit can be expressed as

$$i(t) = \frac{V_c}{Z_0'}\sin(\omega_0' t)\, e^{-\frac{r}{2L}t} \qquad (3\text{-}2)$$

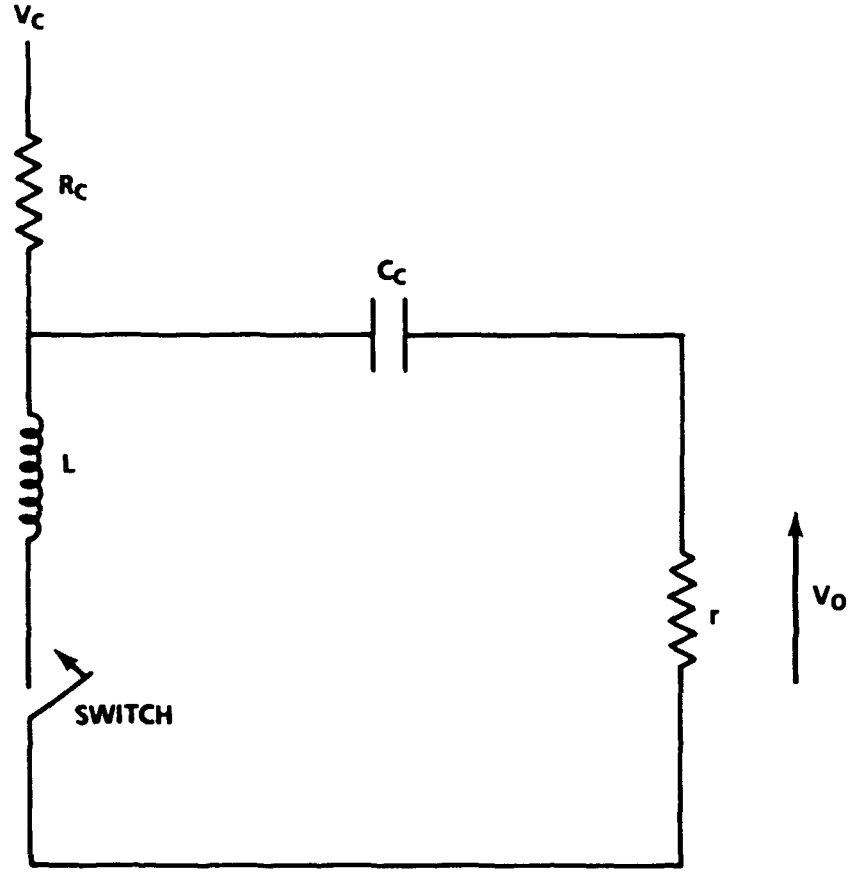

FIGURE 3-1. SCHEMATIC OF THE CLOSING SWITCH TRIGGER CIRCUIT

where $\omega_0' = \omega_0 \sqrt{1 - \frac{1}{4q^2}}$,

$\omega_0 = \frac{1}{\sqrt{LC_c}}$, $q = \frac{\omega_0 L}{r}$,

$Z_0 = \sqrt{\frac{L}{C_c}} = \omega_0 L$, and $Z_0' = \omega_0' L$

Now the output voltage V_o = ir so

$$V_o = \frac{V_c}{q'} \sin(\omega_0' t)\, e^{-\frac{r}{2L}t}, \quad (q \geq \frac{1}{2}) \tag{3-3}$$

where $q' = \frac{\omega_0' L}{r}$

The parameter q is a dimensionless number commonly referred to as the 'quality-factor' of the circuit. When q > ½ the current is oscillatory and the circuit is said to be under-damped. The circuit is over-damped when q < ½, in which case the sine term of Equation (3-3) becomes a hyperbolic sine (sinh) function, i.e.,

$$V_o = \frac{V_c}{q'} \sinh(\omega_0' t)\, e^{-\frac{r}{2L}t}, \quad (q \leq \frac{1}{2}) \tag{3-4}$$

Note that, unlike the piezoelectric signal, the magnitude of the output signal does not depend on the projectile impact velocity v, the tilt θ, or the radius r. Consequently the output is predictable, reliable, and repeatable in a wide variety of experimental conditions.

CIRCUIT EFFICIENCY AND THE OUTPUT VOLTAGE RISE TIME

The circuit is most efficient when q is small, i.e., q « ½. Then the capacitor energy is dissipated rapidly into r. If q » ½ then the circuit oscillates sinusoidally and the energy is slowly dissipated into r. From Equation (3-2) it can be shown that

$$q = \frac{Z_0}{r} = \frac{1}{r}\sqrt{\frac{L}{C_c}} \tag{3-5}$$

Hence L must be minimized to obtain an efficient, low q circuit. For this reason a low inductance capacitance must be used for C_c, e.g., a high frequency disc-ceramic capacitor.

The peak voltage is obtained when $dV_o/dt = 0$. From Equation (3-3) we find that for an over-damped circuit

$$\tanh(\omega_0' t_p) = \frac{2\omega_0' L}{r} = 2q' \qquad (3\text{-}6)$$

$$or \quad t_p = \frac{1}{\omega_0'} \tanh^{-1}(2q')$$

Finally, if q « ½ then the output voltage approaches that of a circuit with an infinite capacitance, i.e., a circuit where voltage is dominated by L and r alone

$$V_o \approx V_c(1 - e^{-\frac{r}{L}t}) \qquad (3\text{-}7)$$

Then the rise time, t_r, defined by the time required for V_o to rise from 10 to 90 percent of its peak value, is $t_r = ln9\ L/r$, i.e., 2.1972 L/r. This expression clearly shows that L must be small for a fast rise time trigger signal. Thus, it is important that L be minimized both to achieve a non-oscillatory signal and a fast rise-time signal.

In the PVDF sensor circuit described in this report, L < 10 nH, C_c = 20 nF, r = 50 Ω, q < 0.01, and the rise time is < 0.6 ns.

PENETRATION TIME

It is difficult to predict the time taken for the projectile to penetrate the PVDF sensor, yet this time is required to predict the duration of the piezoelectric output. The penetration time depends on the properties of the material onto which the sensor is mounted. Typically penetration occurs after a time greater than the thickness of the sensor divided by the velocity, v, e.g., ≈0.5 μs for a 208 μm thick sensor impacted at 500 m/s (Figure 4-2). The combined use of the PVDF trigger circuits, i.e., the use of the piezoelectric signal coupled with the closure switch signal, is discussed in Chapter 4.

CHAPTER 4

THE COMBINATION OF THE PVDF AND CONTACT-CLOSURE TRIGGERS

As described earlier, the projectile may penetrate and short-circuit the PVDF sensor some time after the initial impact, especially if the tilt angle is large. Therefore the trigger was designed as a combination piezoelectric and contact-closure sensor.

Prior to impact the classic piezoelectric signal, shown in Figure 2-4, is obtained. If the projectile penetrates the sensor then a short circuit is formed. A schematic of the combined trigger circuit is shown in Figure 4-1. At the time of penetration current flows through the sensor from the charged capacitor, C_c. In this circuit, C_c was charged to negative voltage so that a positive signal was generated across the terminating load resistor, r. A PVDF sensor, with an active area of 3.0 cm x 1.27 cm, was attached to a ≈15 m length of 50 Ω impedance RG223 coaxial cable. This cable was connected to a coaxial series 20 nF capacitor and then matched with a 50 Ω coaxial terminator (r) at the input to a digital oscilloscope. The capacitor and cable were charged via a 10 kΩ resistor from a 90 V supply.

CIRCUIT COMPONENTS

Stray inductances must be minimized for effective circuit operation. Consequently, the connections to the sensor must be short, close together, and made with relatively thick wires, e.g., ≥ 2 mm diameter. The authors use 15 m to 30 m lengths of RG58 50 Ω cable for these tilt measurement and trigger applications. In noisy signal environments RG223 is used. If long lengths of coaxial cable must be used or if higher frequency signals are to be observed, then RG58 or RG223 are not suitable and a good, low loss cable is recommended. Good quality 50 Ω coaxial terminators should always be used.

The charging capacitor, C_c, was manufactured from a high quality, disc-ceramic capacitor mounted in a copper cylinder and attached to BNC connectors at each end. In this configuration the current passed through the center capacitor and back through the outer copper cylinder and thus formed a coaxial device. Again, lead lengths were kept short. The charging resistor, R_c, can be any type because it is not part of the high frequency circuit.

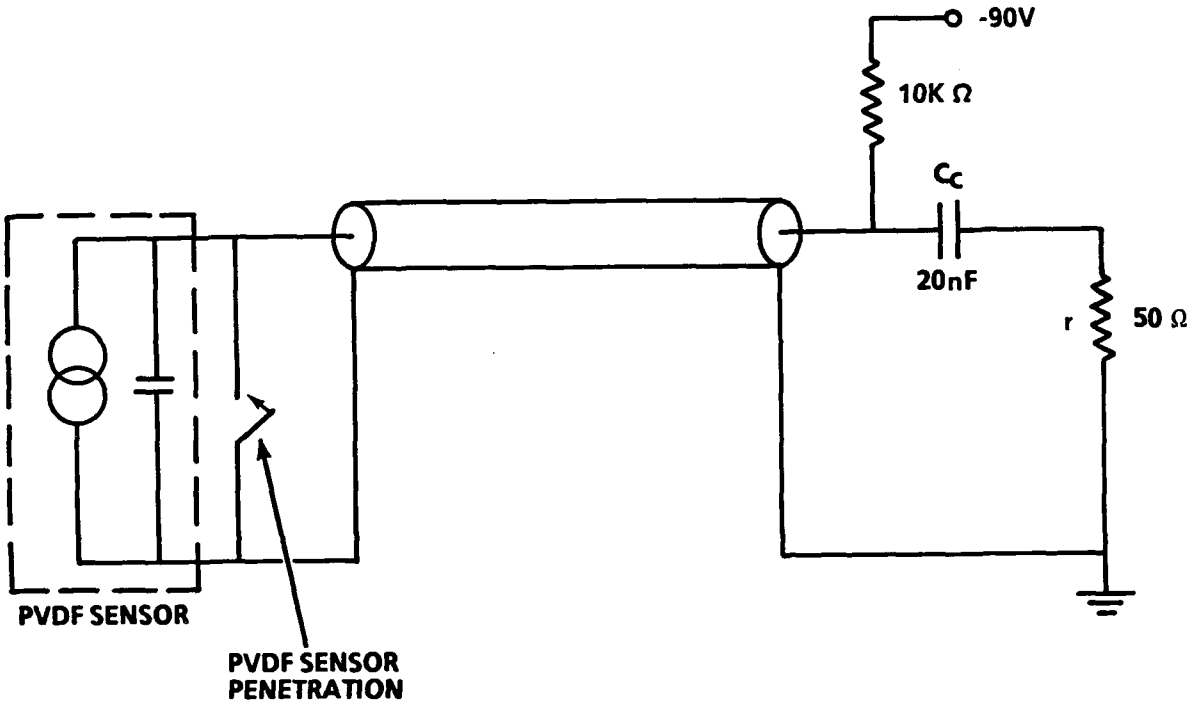

FIGURE 4-1. CIRCUIT OF COMBINED TRIGGER

RESULTS OF THE DUAL TRIGGER CIRCUIT

Typical results are shown in Figure 4-2. The portion of the signal between t≈0 and t≈300 ns corresponds to the piezoelectric output of the sensor. In this experiment the steel-projectile impact velocity was 500 m/s against an explosive target. The tilt was ≈1° as estimated from high-speed framing camera data. The projectile diameter was 9.525 mm.

From these data we would predict a peak voltage of 37.8 V as described earlier for a projectile travelling ***in vacuo***. Clearly this is in reasonable agreement with the peak (for the piezoelectric portion of the signal) of 32 V. At this point the sensor was short-circuited and the closing switch circuit took over.

The piezoelectric signal probably did not reach its peak prior to projectile penetration. For a 1° tilt the total contact time, t_f, would be 381 ns; this is larger than the 300 ns observed here, but the exact tilt angle is not known. Note that the PVDF signal was calculated using calibration data for material poled by the Bauer process, i.e., a different PVDF material; see Equation (2-7). Moreover, the effects of a bow-shock have been ignored. Consequently we feel that while the agreement between the predicted and actual data may be fortuitous, it does suggest that the approximation of using Equation (2-7) predicts a signal of the right magnitude.

For more accurate signal prediction, sensors prepared by the Bauer process must be used or if the Kynar-type sensors are used, calibration data must be independently obtained for each individual sensor over the range of impact pressures to be considered.

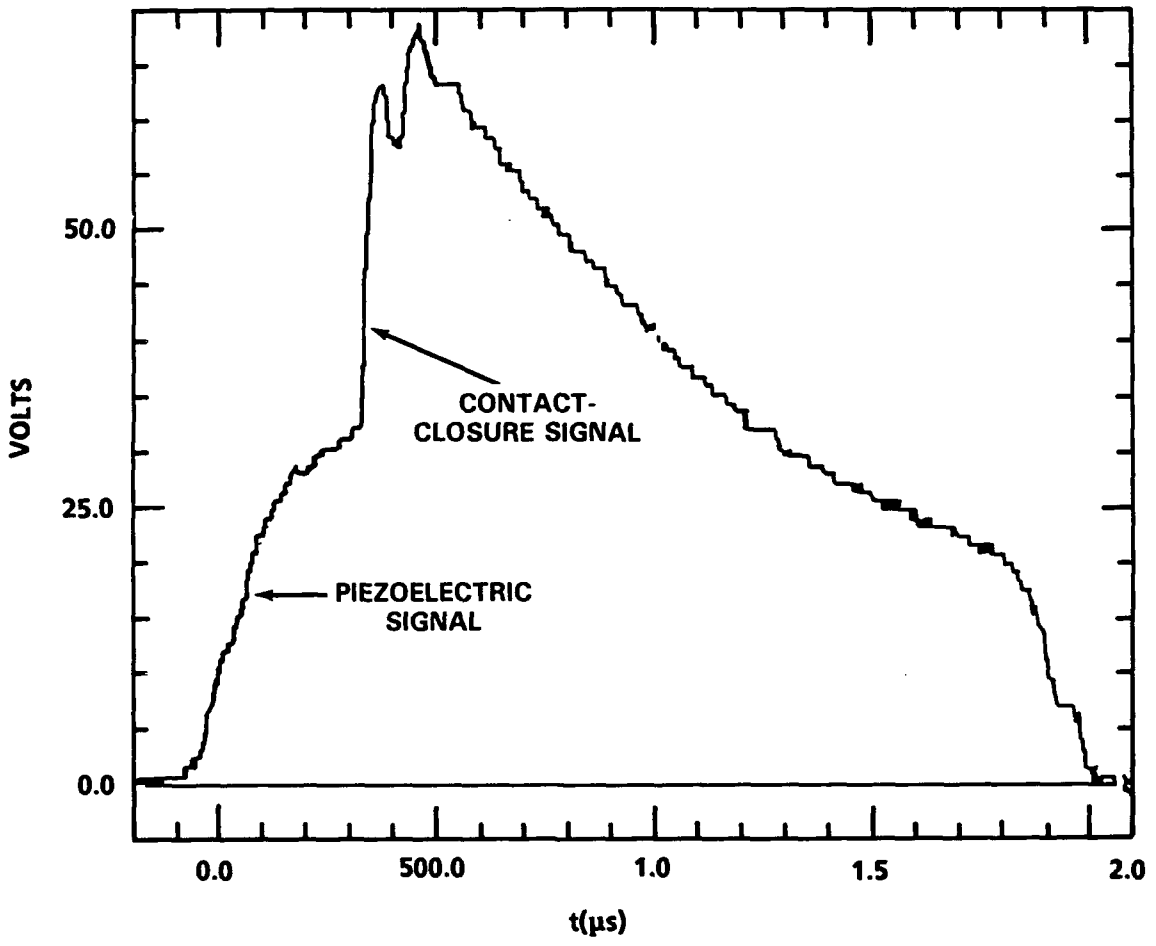

FIGURE 4-2. A TYPICAL DUAL TRIGGER SIGNAL

CHAPTER 5

CONCLUSIONS

We have described a piezoelectric sensor device that provides tilt data for the impact of a projectile against a target ***in vacuo***. Further work is necessary to quantify the change of the tilt signal, if any, due to the effects of bow shocks in air or other gasses. However, applications to date strongly suggest that for use in air at atmospheric pressures the effects of bow shocks are small, and are not serious compared to the advantages of using these PVDF triggers. The tilt signal can be combined with a contact-closure signal to provide a highly reliable and simple trigger that can be used in projectile impact experiments.

The piezoelectric response, i.e., the precursor to the contact-closure signal, gives tilt information from both the magnitude and rise time of the signal. This is followed by the closure-switch signal which has a fast rise time, < 1 ns, and a magnitude that can be accurately predicted. The closure signal is independent of the projectile's velocity, tilt, impact pressure, and radius.

Finally, the sensor is inexpensive and easy to manufacture from readily available components.

REFERENCES

1. F. Bauer, "Ferroelectric Properties and Shock Response of a Poled PVF_2 Polymer," Shock Waves in Condensed Matter, 1986, Plenum Press, N.Y., N.Y. 10013.

2. R. A. Graham, F. Bauer, L. M. Lee, R. P. Reed, "The Standardized Bauer Piezoelectric Polymer Shock Gauge," Shock Wave Compression of Condensed Matter, Proceedings, Washington State University, Pullman, WA, Sep 1988.

3. L. M. Moore, et al., "Standardized Piezoelectric Polymer (PVDF) Gauge for Detonator Response Measurements," Third International High Dynamic Pressure Symposium, France, 5-9 Jun 1989.

APPENDIX A

DESCRIPTION OF THE PROJECTILE IMPACT EXPERIMENTS

For this work, the dual-trigger source was used to provide trigger signals in two series of projectile impact experiments. In both applications the source never failed to perform as expected.

FRAGMENT IMPACT EXPERIMENTS

A reliable trigger was needed for a series of fragment impact experiments. These experiments were designed to study the fragment impact sensitivity of explosives munitions. The dual trigger/tilt sensor was incorporated into these experiments to evaluate its performance.

The general arrangement is shown in Figure A-1. PVDF sensors were used to detect the arrival of the projectile on the front surface of the target. The charges were 76.2 mm in diameter by 76.2 mm long cast Pentolite, density $\approx$1.67 g/cm^3. The charges were confined along their length in brass tubes of 6.4 mm wall thickness, and at their rear surface with a steel witness block 127 mm diameter by 76 mm thick. In two tests, the front surface of the charge was not covered, so that the projectile impacted it directly; see Table 1. In the other tests, the front surface was covered by a 4.8 mm thick mild steel plate, held in direct contact with the test charge; the projectile velocities always exceeded those needed to penetrate the plate.

In these experiments, the Kynar PVDF sensor was adhered to the bare face of the explosive or the front surface of the cover plate with ordinary double-sided adhesive tape (0.003 in. thick, nominal). A short length of twisted leads connected the sensor and RG58 coaxial cable. The circuitry used is described in Figure 4-1. Nicolet 4094 oscilloscopes with 4180 plug-ins, running at 5 ns per point, recorded the sensor data. Figure A-2 shows the location of the sensor.

Flat-nosed steel projectiles, having masses between 60 g and 80 g and lengths of 36 mm, were fired at the targets by a 20 mm rifled gun. The projectile diameter was varied from 9.5 to 19 mm. High-speed photography was used to measure the projectile velocities, V, and the flatness of their impacts on the target.

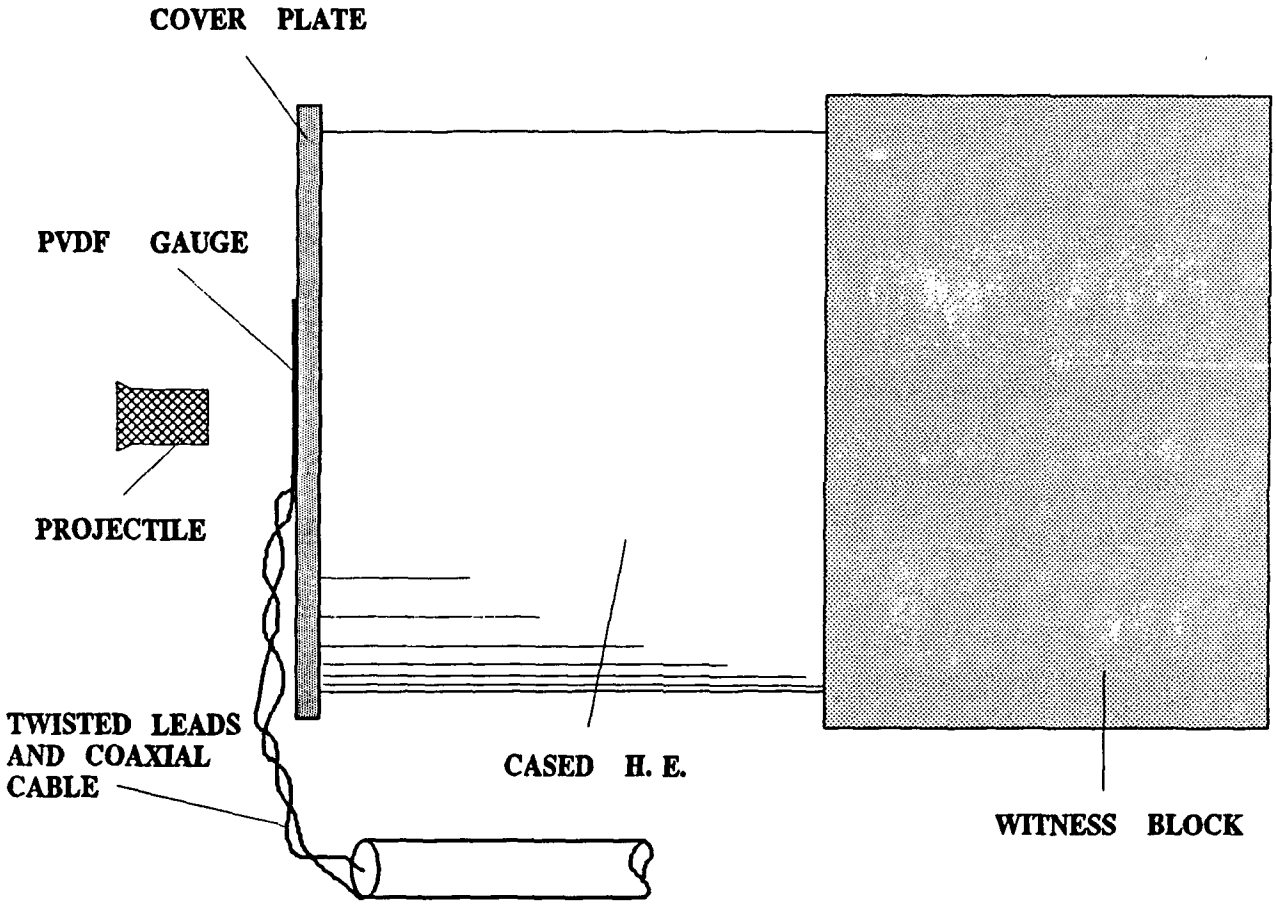

FIGURE A-1. FRAGMENT IMPACT EXPERIMENT

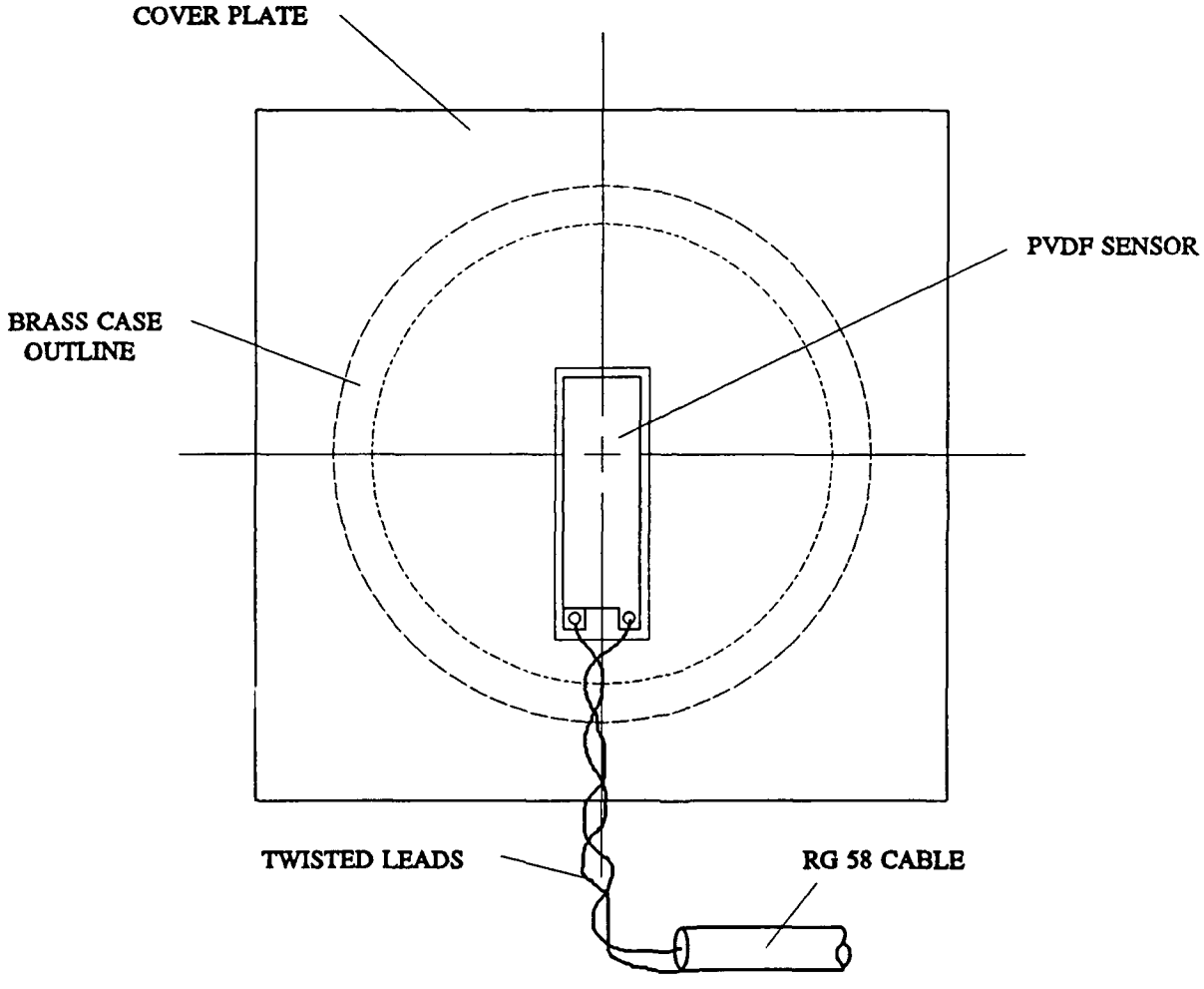

FIGURE A-2. PLACEMENT OF PVDF SENSOR

DISTRIBUTION

	Copies
Chief of Naval Research	
Attn: ONR 1132P (R. Miller)	1
ONT 20T (L. V. Schmidt)	1
ONT 213 (D. Siegel)	1
ONT 23 (A. J. Faulstich)	1
ONT 232 (D. Houser)	1
800 N. Quincy Street, BCT 1	
Arlington, VA 22217-5000	
OUSDRE/R&AT-MST	
Attn: R. Siewart	1
The Pentagon	
Washington, DC 20301	
OUSDRE/TWP-NW&M	
Attn: D. Anderson	1
The Pentagon	
Washington, DC 20301	
OUSDRE/TWP--OM	
Attn: G. Kopcsak	1
The Pentagon	
Washington, DC 20301	
USD(A)/DDRE (R/AT/ET)	
Staff Specialist for Weapons Technology	
Attn: F. Menz	1
The Pentagon	
Washington, DC 20301	
OASN/RE&S	
Attn: Surface Warfare	1
Air Warfare	1
Subs/ASW	1
Navy Department	
Washington, DC 20301	

	Copies
Chairman	
Department of Defense Explosives Safety Board	
Attn: 6-A-145	1
DDESB-KT	1
Hoffman Building 1	
2461 Eisenhower Avenue	
Alexandria, VA 22331	
Chief of Naval Operations	
Attn: OP-098	1
OP-981	1
OP-982	1
OP-983	1
OP-987	1
OP-02T	1
OP-22	1
OP-225	1
OP-32	1
OP-35	1
OP-37	1
OP-374	1
OP-501	1
OP-502	1
OP-503	1
OP-72	1
OP-74	1
OP-75	1
Navy Department	
Washington, DC 20350	
Commander	
Space and Naval Warfare Systems Command	
Attn: SPAWAR-05	1
Washington, DC 20363-5100	

DISTRIBUTION (Cont.)

		Copies
Commander		
Naval Sea Systems Command		
Attn:	SEA-05R	1
	SEA-55	1
	SEA-55X	1
	SEA-55X1	1
	SEA-55X2	1
	SEA-55Y	1
	SEA-66U	1
	SEA-62	1
	SEA-62Y	1
	SEA-62Z	1
	SEA-63	1
	SEA-63D	1
	PMS-402	1
	PMS-406	1
	PMS-407	1
Washington, DC 20362-5105		
Commander		
Naval Air Systems Command		
Attn:	AIR-5004	1
	AIR-51623	1
	AIR-540	1
	AIR-5404	1
	AIR-93	1
	AIR-932F	1
	AIR-932H	1
	AIR-932K	1
	AIR-932T	1
	PMA-242	1
	Technical Library	1
Washington, DC 20361		
Commander		
Naval Surface Warfare Center		
Carderock Division		
Attn:	Technical Library	1
	Code 17	1
	Code 172	1
	Code 1740.3 (R. Garrison)	1
	Code 1740.4 (S. Wang)	1
	Code 175 (W. Sykes)	1
	Code 1750.2 (W. Conley)	1
	Code 1740.2 (F. Fisch)	1
Bethesda, MD 20084		

		Copies
Commander		
David Taylor Research Center		
Attn:	Code 177	1
	Technical Library	1
Portsmouth, VA 20375		
Commanding Officer		
Naval Research Laboratory		
Attn:	Technical Library	1
Washington, DC 20375		
Commanding Officer		
Naval Surface Warfare Center		
Dahlgren Division		
Coastal Systems Station		
Attn:	Technical Library	1
Panama City, FL 32407-5000		
Commander		
Naval Undersea Warfare Division		
Attn:	Technical Library	1
Newport, RI 02841-5047		
Commander		
Naval Air Warfare Center		
Weapons Division		
Attn:	Code 3917	1
	Code 38 (R. Derr)	1
	Code 389 (T. Boggs)	1
	Code 32	1
	Code 3205	1
	Code 3208	1
	Code 326	1
	Code 3261	1
	Code 3263	1
	Code 3264	1
	Code 3265	1
	Code 3266	1
	Code 327	1
	Code 381	1
	Code 385	1
	Code 3850	1
	Code 3853	1
	Code 3891 (J.Covino)	1
	Code 39	1
	Technical Library	1
China Lake, CA 93555-6001		

DISTRIBUTION (Cont.)

	Copies
Commander Naval Surface Warfare Center Indian Head Division	
Attn: Code 2730D	1
Technical Library	1
J. Chang	1
P. Dendor	1
L. Newman	1
Indian Head, MD 20640-5000	
Commander Center for Naval Analyses	
Attn: Technical Library	1
2000 Suitland Road Washington, DC 20390-5140	
Superintendent Naval Postgraduate School	
Attn: Library	1
Monterey, CA 93940	
President Naval War College	
Attn: Technical Library	1
Newport, RI 02841	
Commanding Officer Naval Amphibious Base, Coronado	
Attn: RDT Officer	1
SEAL Team	1
Underwater Demolition Team	1
San Diego, CA 92155	
Commanding Officer Naval Amphibious Base Little Creek	
Attn: RDT Officer	1
Norfolk, VA 23511	
Commanding Officer Naval Explosive Ordnance Disposal Technology Center	
Attn: Technical Library	1
Indian Head, MD 20640	
Commander Pacific Missile Test Center	
Attn: Code 2145	1
Point Mugu, CA 93042	
Commanding Officer SEAL Team 2	
FPO New York, NY 09501-4633	1
Commander Naval Undersea Warfare Division	1
Keyport, WA 98345-0580	
Commander Naval SurfaceWarfare Center Port Hueneme Division	1
Port Hueneme, CA 93043-5007	
Commander Naval Weapons Evaluation Facility Kirtland Air Force Base	
Albuquerque, NM 87117	1
Commander Naval Surface Warfare Center Crane Division	
Attn: Code 3031 (E. Neal)	1
Code 50D (A. Norris)	1
Code 505 (J. E. Short)	1
Code 90 (A. E. Whitner)	1
Crane, IN 47522-5000	
Commanding Officer Naval Weapons Station	
Attn: Code 321 (M. Bucher)	1
Concord, CA 94520-5000	
Officer in Charge Naval Surface Warfare Center Indian Head Division Yorktown Detachment	
Attn: Code 470A	1
Library	1
Yorktown, VA 23691-5110	
Director Defense Nuclear Agency	
Attn: Technical Library	1
Washington, DC 20305	

DISTRIBUTION (Cont.)

	Copies
Defense Science Board Attn: C. Fowler The Pentagon Washington, DC 20301	1
Director Defense Research and Engineering Attn: Library Washington, DC 20305	1
Director Defense Advanced Research Projects Agency Attn: Library 1400 Wilson Blvd. Arlington, VA 22209	1
Institute for Defense Analyses Attn: Technical Library 1801 N. Beauregard Street Alexandria, VA 22311	1
Commanding General Marine Corps Development and Education Command Attn: Library Marine Corps Landing Force Development Center Quantico, VA 22134	1
Army Armament Munitions and Chemical Command Attn: DRSAR-IRC DRSAR-LEM (R. Freeman) DRSAR-SF (R. Young) Rock Island, IL 61299-6000	1 1 1
Army Armament Research and Development Command Attn: Technical Library Dover, NJ 07801	1
Redstone Arsenal Army Missile Command Attn: Chief, Documents D. Dreitzler Redstone Arsenal, AL 35809	1 1
Army Ballistic Research Laboratory Attn: SLC-BR-TB-EE SLCRBR-IB-I (P. Kaste) V. Boyle O. Blake R. Frey G. Melani M. Chawla J. Trimble Technical Library Aberdeen Proving Ground Aberdeen, MD 21005-5066	1 1 1 1 1 1 1 1 1
Commander Officer Harry Diamond Laboratory Attn: Library 2800 Powder Mill Road Adelphi, MD 20783	1
Army Environmental Hygiene Agency Attn: HSHB-EA-A Aberdeen Proving Ground Aberdeen, MD 21005	1
Army Medical Bioengineering Research and Development Laboratory Attn: J. Barkeley Fort Dietrick, MD 21701	1
Commander Army Research Office Attn: G. R. Husk P. O. Box 12211 Research Triangle Park, NC 27709-2211	1
Army Toxic and Hazardous Materials Agency Attn: DRXTH-TE-D Aberdeen Proving Ground Aberdeen, MD 21005	1
Commander Army Chemical Research, Development and Engineering Center Attn: SMCCR-DDP Aberdeen Proving Ground, MD 21010-5423	1

DISTRIBUTION (Cont.)

	Copies
Wright Laboratory/Armament Directorate	
Attn: WL/MNME	1
WL/MNMW	1
WL/MNOI	1
WL/MNME (G. Glenn)	1
WL/MNMF (R.Mabrey)	1
WL/MNME (R. McKinney)	1
WL/MNMW (J. Foster)	1
Eglin Air Force Base, FL 32542-5000	
Air Force Office of Scientific Research	
Attn: T. Matusko	1
Bolling Air Force Base	
Washington, DC 20332	
University of California	
Lawrence Livermore National Laboratory	
Attn: Technical Library	1
M. Finger	1
C. M. Tarver	1
E. Lee	1
P. Urtiew	1
J. D. Hallquist	1
L. M. Erickson	1
E. James	1
P. O. Box 808	
Livermore, CA 94550	
Los Alamos National Laboratory	
Attn: J. Repa	1
M. J. Urizar	1
S. W. Peterson	1
L. Smith	1
C. Forest	1
C. Morris	1
A. W. Campbell	1
R. Engelke	1
P. C. Crawford	1
Los Alamos, NM 87545	
Sandia National Laboratories	
Attn: Technical Library	1
P. O. Box 969	
Livermore, CA 94550-0096	
Sandia National Laboratories	
Attn: Structural and Shock Chemistry, Division 1153 (Mark U. Anderson)	1
Albuquerque, NM 87185-5800	
Argonne National Laboratory	
Attention Records Control for:	
Richard Anderson	1
Technical Library	1
9700 South Cass Avenue	
Argonne, IL 60439	
The Johns Hopkins University Applied Physics Laboratory	
Chemical Propulsion Information Agency	
Attn: T. W. Christian	1
Johns Hopkins Road	
Laurel, MD 20707	
The Johns Hopkins University Applied Physics Laboratory	
Attn: Technical Library	1
Johns Hopkins Road	
Laurel, MD 20707	
New Mexico Institute of Mining Technology	
Attn: Code TERA (J. Joyner)	1
Technical Library	1
Socorro, NM 87801	
Applied Research Laboratory	
Pennsylvania State University	
Attn: Library	1
E. Lizka	1
P. O. Box 30	
University Park	
State College, PA 16801	
Defense Technical Information Center	
Cameron Station	
Alexandria, VA 22304-6142	12

DISTRIBUTION (Cont.)

	Copies
Royal Armament Research and Development Establishment	
Attn: Library	1
B. Hammant	1
P. Hart	1
P. Haskins	1
Fort Halstead, Sevenoaks, Kent	
United Kingdom	
Atomic Weapons Establishment	
Attn: Library	1
H. R. James	1
Foulness Island	
Essex SS3 9XE	
United Kingdom	
Royal Ordnance Plc	
Attn: Library	1
P. Lee	1
R. H. Martin	1
Westcott, Aylesbury	
Buckinghamshire	
HP18 ONZ	
United Kingdom	
The British Embassy	
Attn: P. Jones	1
British Defence Staff	
3100 Massachusetts Avenue, N.W.	
Washington, DC 20008	
Materials Research Laboratory	
Attn: M. Chick	1
P. O. Box 50	
Ascot Vale, Victoria 3032	
Australia	
Société Nationale des Poudres et Explosifs	
Attn: J. Brunet	1
R. Rat	1
D. Idelot	1
Centres de Recherches du Bouchet	
B.P. 2-91710	
Vert-le-Petit	
France	

	Copies
Institute de Saint-Louis	
Attn: F. Bauer	1
12 rue de l'industrie	
68300 Saint Louis	
France	
Advanced Technology and Research, Inc.	
Attn: S. Jacobs	1
W. Pickler	1
T. P. Liddiard	1
J. W. Watt	1
Laurel Technology Center	
14900 Sweitzer Lane	
Laurel, MD 20707	
TRW	
Attn: R. Church	1
San Bernadino, CA 92401	
Aerojet Ordnance and Manufacturing Company	
Attn: G. Chin	1
9236 East Hall Road	
Downey, CA 90241	
Vanderbilt University	
Attn: A. Mellor	1
Nashville, TN 37235	
Lockheed Missiles and Space Company	
Attn: R. Hodges	1
J. Smith	1
P. O. Box 504	
Sunnyvale, CA 94086	
Hercules Incorporated Rocket Center	
Attn: G. Williams	1
P. O. Box 210	
Rocket Center, WV 26726	

DISTRIBUTION (Cont.)

	Copies
Hercules	
Attn: M. Klakken	1
M. Berger	1
L. Losee	1
T. Speed	1
Bacchus Works	
Magna, UT 84044-0098	
Thiokol Corporation	
Tactical Operations	
Attn: D. Jeff Jones, Materials and Process Development	1
Huntsville Division	
P. O. Box 400006	
Huntsville, AL 35815-1506	
Ktech Corporation	
901 Pennsylvania Avenue	
Attn: Larry Lee	1
Albuquerque, NM 87110	
Alliant Techsystems, Inc.	
Attn: K. L. Christianson	1
J. L. Houlton	1
G. Johnson	1
7225 Northland Drive	
Brooklyn Park, MN 55428	
Library of Congress	
Attn: Gift and Exchange Division	1
Washington, DC 20540	
Société Nationale des Poudres et Explosifs	
Attn: J. Brunet	1
R. Rat	1
D. Idelot	1
Centres de Recherches du Bouchet	
B.P. 2-91710	
Vert-le-Petit	
France	
Institute de Saint-Louis	
Attn: F. Bauer	1
12 rue de l'industrie	
68300 Saint Louis	
France	

Internal distribution:		Copies
E231		2
E232		3
E342		1
G13	(D. L. Dickinson)	1
G13	(T. Wasmond)	1
G22	(W. H. Holt)	1
	(W. Mock)	1
	(S. S. Waggener)	1
R10		1
R101		1
R10	(R. R. Bernecker)	1
R10A	(C. Dickinson)	1
R10B	(H. S. Haiss)	1
R10A1		1
R10A2		1
R11		1
R12		1
R12	(B. A. Baudler)	1
	(B. C. Glancy)	1
	(L. C. Hudson)	1
	(G. Laib)	1
	(L. L. Mensi)	1
	(L. J. Montesi)	1
	(P. F. Spahn)	1
	(T. Spivak)	1
R13		1
R13	(K. D. Ashwell)	1
	(R. N. Baker)	1
	(R. D. Bardo)	1
	(A. Brown)	1
	(C. S. Coffey)	1
	(J. Davis)	1
	(D. L. Demske)	1
	(J. W. Forbes)	1
	(R. H. Guirguis)	1
	(P. K. Gustavson)	5
	(R. N. Hay)	1
	(H. D. Jones)	1
	(K. Kim)	1
	(R. J. Lee)	1
	(W. W. Lee)	1
	(E. R. Lemar)	1
	(P. J. Miller)	1
	(C. T. Richmond)	1
	(H. W. Sandusky)	1
	(G. T. Sutherland)	1
	(D. G. Tasker)	5
	(W. H. Wilson)	5

DISTRIBUTION (Cont.)

		Copies
Internal distribution (Cont.):		
	(D. L. Woody)	1
	(F. J. Zerilli)	1
R14		1
R14	(J. W. Koenig)	1
R15		1
R15	(S. Collignon)	1
R42	(R. Dewitt)	1
U10	(W. Wassmann)	1
U11	(R. Plenge)	1
	(D. Hinely)	1
U12	(C. Smith)	1
	(W. Hinckley)	1
U32	(G. Parrent)	1
U43	(L. Lipton)	1

REPORT DOCUMENTATION PAGE

Form Approved OMB No. 0704-0188

1. AGENCY USE ONLY *(Leave blank)*	2. REPORT DATE	3. REPORT TYPE AND DATES COVERED
	November 1991	

4. TITLE AND SUBTITLE

A PVDF Trigger and Tilt Detector for Projectile Impact Experiments

5. FUNDING NUMBERS

6. AUTHOR(S)

Douglas G. Tasker, Paul K. Gustavson, and William H. Wilson

7. PERFORMING ORGANIZATION NAME(S) AND ADDRESS(ES)

Naval Surface Warfare Center
10901 New Hampshire Avenue
Silver Spring, MD 20903-5000

8. PERFORMING ORGANIZATION REPORT NUMBER

NAVSWC TR 91-640

9. SPONSORING/MONITORING AGENCY NAME(S) AND ADDRESS(ES)

Office of Chief of Naval Research
Code ONT 232
800 N. Quincy Street, BCT 1
Arlington, VA 22217-5000

10. SPONSORING/MONITORING AGENCY REPORT NUMBER

11. SUPPLEMENTARY NOTES

12a. DISTRIBUTION/AVAILABILITY STATEMENT

Approved for public release; distribution is unlimited.

12b. DISTRIBUTION CODE

13. ABSTRACT *(Maximum 200 words)*

A sensor is described which is used as a trigger source for shock wave and projectile impact experiments, and also measures projectile tilt. The piezoelectric device uses plyvinylidene di-fluoride (PVDF) as the sensor. Two independent signals are produced: one a piezoelectric signal, the other a contact-closure signal. This duality significantly improves the reliability of the trigger. Full experimental details, theoretical analysis, and results are provided. To date this trigger has been used successfully by the authors many times without a single failure.

14. SUBJECT TERMS

Piezoelectricity	PVDF	Oscilloscope trigger	Closing switch
Polyvinylidene di-fluoride	PVF_2	Projectile impact	Circuit analysis
	Shock waves	Projectile tilt	Circuit inductance

15. NUMBER OF PAGES

48

16. PRICE CODE

17. SECURITY CLASSIFICATION OF REPORT	18. SECURITY CLASSIFICATION OF THIS PAGE	19. SECURITY CLASSIFICATION OF ABSTRACT	20. LIMITATION OF ABSTRACT
UNCLASSIFIED	UNCLASSIFIED	UNCLASSIFIED	SAR

GENERAL INSTRUCTIONS FOR COMPLETING SF 298

The Report Documentation Page (RDP) is used in announcing and cataloging reports. It is important that this information be consistent with the rest of the report, particularly the cover and its title page. Instructions for filling in each block of the form follow. It is important to ***stay within the lines*** to meet ***optical scanning requirements***.

Block 1. Agency Use Only *(Leave blank)*.

Block 2. Report Date. Full publication date including day, month, and year, if available (e.g. 1 Jan 88). Must cite at least the year.

Block 3. Type of Report and Dates Covered. State whether report is interim, final, etc. If applicable, enter inclusive report dates (e.g. 10 Jun 87 - 30 Jun 88).

Block 4. Title and Subtitle. A title is taken from the part of the report that provides the most meaningful and complete information. When a report is prepared in more than one volume, repeat the primary title, add volume number, and include subtitle for the specific volume. On classified documents enter the title classification in parentheses.

Block 5. Funding Numbers. To include contract and grant numbers; may include program element number(s), project number(s), task number(s), and work unit number(s). Use the following labels:

C	- Contract	PR	- Project
G	- Grant	TA	- Task
PE	- Program Element	WU	- Work Unit Accession No.

BLOCK 6. Author(s). Name(s) of person(s) responsible for writing the report, performing the research, or credited with the content of the report. If editor or compiler, this should follow the name(s).

Block 7. Performing Organization Name(s) and Address(es). Self-explanatory.

Block 8. Performing Organization Report Number. Enter the unique alphanumeric report number(s) assigned by the organization performing the report.

Block 9. Sponsoring/Monitoring Agency Name(s) and Address(es). Self-explanatory.

Block 10. Sponsoring/Monitoring Agency Report Number. *(If Known)*

Block 11. Supplementary Notes. Enter information not included elsewhere such as: Prepared in cooperation with...; Trans. of...; To be published in.... When a report is revised, include a statement whether the new report supersedes or supplements the older report.

Block 12a. Distribution/Availability Statement. Denotes public availability or limitations. Cite any availability to the public. Enter additional limitations or special markings in all capitals (e.g. NOFORN, REL, ITAR).

DOD	- See DoDD 5230.24, "Distribution Statements on Technical Documents."
DOE	- See authorities.
NASA	- See Handbook NHB 2200.2
NTIS	- Leave blank.

Block 12b. Distribution Code.

DOD	- Leave blank.
DOE	- Enter DOE distribution categories from the Standard Distribution for Unclassified Scientific and Technical Reports.
NASA	- Leave blank.
NTIS	- Leave blank.

Block 13. Abstract. Include a brief ***(Maximum 200 words)*** factual summary of the most significant information contained in the report.

Block 14. Subject Terms. Keywords or phrases identifying major subjects in the report.

Block 15. Number of Pages. Enter the total number of pages.

Block 16. Price Code. Enter appropriate price code ***(NTIS only)***

Blocks 17.-19. Security Classifications. Self-explanatory. Enter U.S. Security Classification in accordance with U.S. Security Regulations (i.e., UNCLASSIFIED). If form contains classified information, stamp classification on the top and bottom of the page.

Block 20. Limitation of Abstract. This block must be completed to assign a limitation to the abstract. Enter either UL (unlimited) or SAR (same as report). An entry in this block is necessary if the abstract is to be limited. If blank, the abstract is assumed to be unlimited.